Mon. Not. R. astr. Soc. (1976) **177**, 463–472.

AN APERTURE SYNTHESIS STUDY OF THE IRREGULAR GALAXY HOLMBERG II

Geoffrey A. Cottrell

Mullard Radio Astronomy Observatory, Cavendish Laboratory, Madingley Road, Cambridge CB3 oHE

(Received 1976 March 29)

SUMMARY

The Cambridge Half-Mile telescope has been used to map the H I distribution and velocity field of Ho II with an angular resolution of $2' \times 2'{\cdot}1$ and a velocity resolution 16 km s^{-1}. The H I disc is 25–50 per cent larger than the Holmberg dimensions and the H I surface density is strongly peaked at the centre. The rotational velocity field is regular out to a radius 7 kpc and the total mass is $(4 \pm 1) \times 10^9 M_\odot$. The internal dynamics of two bright central condensations imply that these are gravitationally bound, consistent with the fact that they are near sites of star formation. The hydrogen structure of Ho II is similar to that of the irregular galaxy IC 10.

1. INTRODUCTION

Holmberg II (Plate I) was discovered by Holmberg (1950) during his survey of galaxies in the M81 group. It has the appearance of a Magellanic irregular, and was classified as type I..9 by de Vaucouleurs & de Vaucouleurs (1964). There is a good photograph of Ho II in *The Hubble Atlas of Galaxies* (Sandage 1961) showing many H II regions and resolved stars brighter than $M_{pg} \approx -4{\cdot}1$. The bluest and very red supergiant stars have been listed by Sandage & Tammann (1974) who also derive a distance of 3·22 Mpc. The H I spectrum has been measured by Rogstad, Rougoor & Whiteoak (1967) who also found Ho II to be a continuum radio source of flux density 400 mJy at 1420 MHz. Recent measurements by Dean & Davies (1975) have indicated an H I mass of $8{\cdot}4 \times 10^8 M_\odot$ and a total indicative mass of $1{\cdot}2 \times 10^9 M_\odot$. Ho II was selected for observation with the Half-Mile telescope because it has (a) a high H I flux and could therefore be mapped with high resolution and a good signal-to-noise ratio, and (b) regions of star formation on angular scales 1′–2′, a size comparable with the beam. A study of star formation in an optically structureless galaxy is interesting because there is no obvious spiral density pattern to ' trigger ' the star formation.

2. THE OBSERVATIONS AND REDUCTION TECHNIQUE

Observations of Ho II were made with the Cambridge Half-Mile telescope (Baldwin *et al.* 1971) in the period 1975 March–1976 January and consisted of a series of 12-hr observations at each of 48 interferometer spacings, the incremental spacing being 6·1 m. The smallest spacing was 12·2 m (58 λ), so source structure larger than 1° will be progressively more attenuated by the telescope response, and no structure on scales $\gtrsim 3°{\cdot}8$ was recorded. The synthesized beam was $2' \times 2'{\cdot}1$,

corresponding to 1·9 × 2·0 kpc at the assumed distance (3·22 Mpc) of the galaxy. The telescope was calibrated by observations of 3C 309.1, the flux density of which was taken as 7·9 Jy (Kellermann, Pauliny-Toth & Williams 1969). The system noise temperature was 120 K.

Hydrogen-line data were sampled with the 160-channel cross-correlation receiver, having a total bandwidth of 2 MHz. The channel separation used corresponded to a velocity difference of 13·1 km s^{-1}, and the full-width at half-maximum (FWHM) of the synthesized response was 15·8 km s^{-1}. Continuum radiation was monitored on the 10-MHz broadband receiver, the centre frequency of both receivers being 1420·0 MHz. Single-channel maps having velocities in the heliocentric radial velocity interval 92–237 km s^{-1} showed H I emission, and the remaining maps (in the velocity ranges −131 to 92 and 237–289 km s^{-1}) were averaged to provide a map of the continuum emission. This continuum map was subtracted from each single-channel map, thereby generating a series of 11 maps

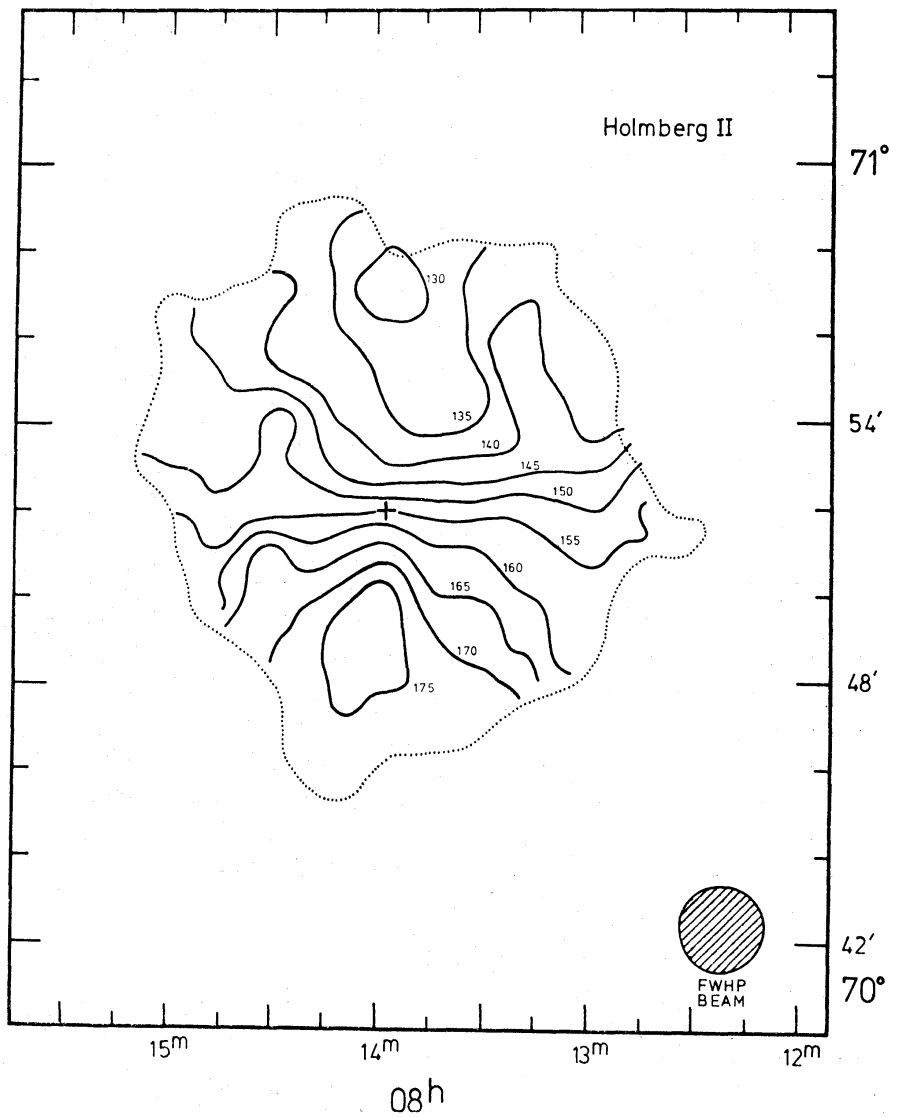

FIG. 2. *The velocity field in Ho II. Contours are lines of constant radial velocity in km s^{-1} with respect to the Sun. The + marks the position of the dynamical centre (see Section 3.2). The dotted line is the faint 124 K km s^{-1} H I contour taken from the integrated H I map (Fig. 1). Rms noise is about 3 km s^{-1}.*

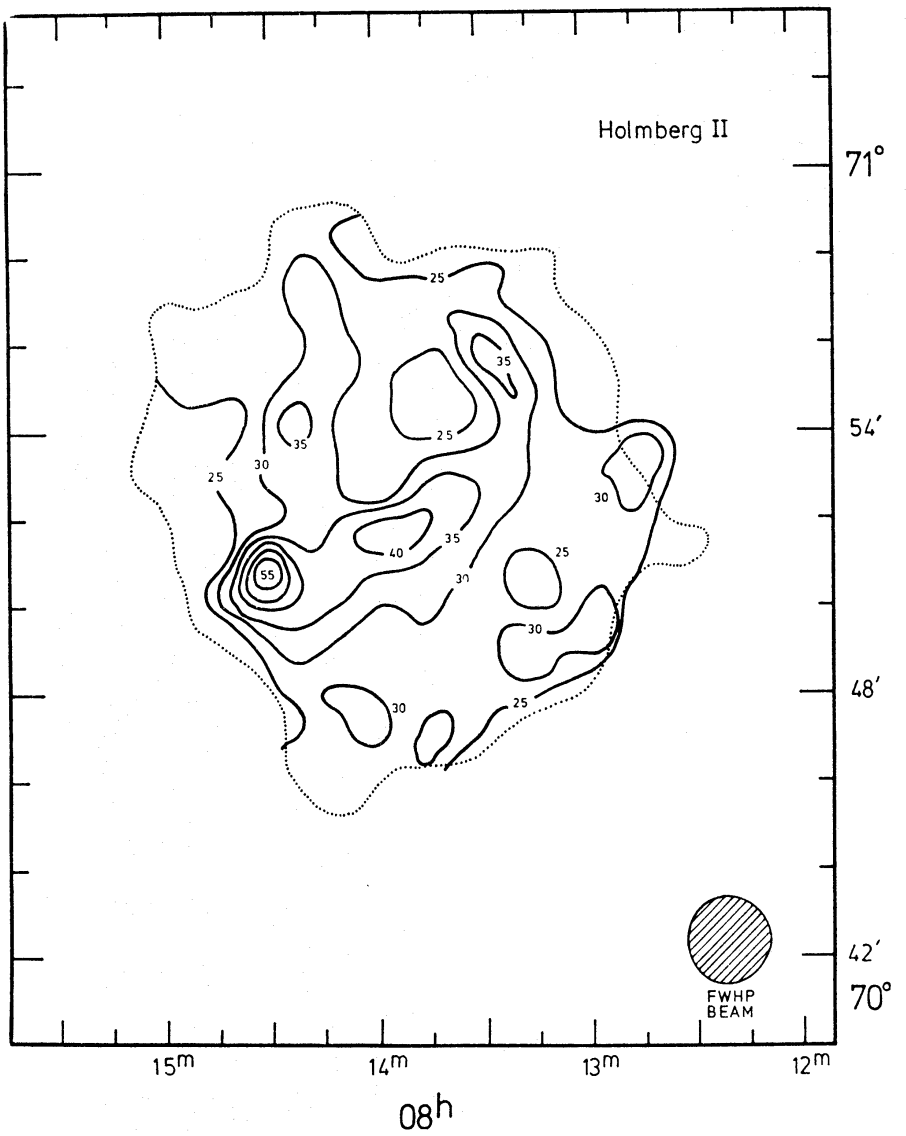

FIG. 3. *The velocity FWHM map. The interval is* 5 *km* s^{-1} *and the outer dotted line is as in Fig.* 2.

of the H I emission alone. A profile-fitting programme was used to produce three final maps, (i) the integrated H I map (Plate I and Fig. 1) made by setting to zero all points on the single-channel maps less than 1·5 × the measured rms noise (24 mJy) and adding, (ii) the radial velocity map (Fig. 2), constructed by finding the mean of the two velocities at which the profile at each grid point had dropped to half its peak value, and (iii) the profile FWHM map (Fig. 3) constructed by finding the full-width at half-power of the profile at each grid point. This map will be subject to beam-smoothing on a scale 2′. These data were reduced on the IBM 370/165 of the University Computer Laboratory.

3. RESULTS

3.1 *The hydrogen distribution*

The dimensions of the H I distribution at a surface density of $2{\cdot}3 \times 10^{20}$ atom cm^{-2} are 15′ × 12′·7 along the major (pa 175°) and minor axes respectively, between

25 and 50 per cent larger than the optical dimensions of $10' \times 10'$ at a surface brightness of 26·5 mag (arcsec)$^{-2}$ (Holmberg 1950). The apparent axial ratio, ϵ_A, of the distribution is 0·84, implying an inclination of $i = 32°$ if Ho II were a thin circular disc. The distribution is peaked towards the centre of the galaxy (*cf.* Fig. 1 and Plate I) which is dominated by two bright H I condensations (designated I and II in order of increasing RA). Condensations I, II and two ' holes ' in the H I are at a common radius $r = 2' \pm 0'{\cdot}5$ from the dynamical centre. H I masses and dimensions of I and II are given in Table I. The peak brightness temperatures

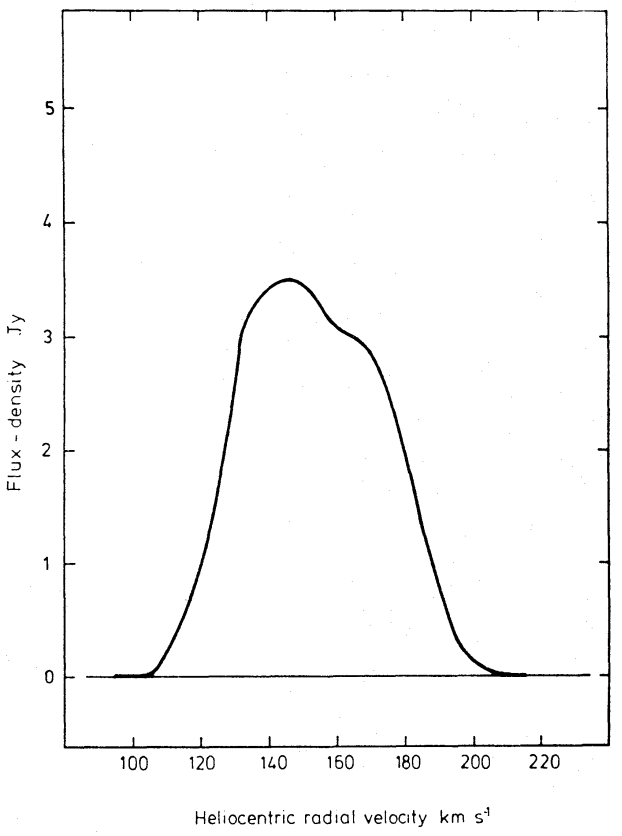

FIG. 4. *The integrated spectrum of H I emission constructed with flux density measurements made on the shortest baseline used* (58 λ). *The adopted systemic velocity of Holmberg II is* $V_s = 155 \pm 5$ *km* s^{-1}, *and the full-width at half-maximum is* 57 ± 3 *km* s^{-1}.

observed in I and II are 24 K. If the condensations are smaller than the beam, the optical depth may be greater than 1. In this case, the measured H I masses (Section 4) are *lower limits*, but no corrections for self-absorption have been applied in this paper.

Fig. 4 shows the H I emission spectrum measured for Ho II; it was constructed by measuring the total H I flux density in each channel at the shortest baseline (58 λ) of the survey. The overall H I mass (M_{HI}) was found to be $(4{\cdot}8 \pm 0{\cdot}2) \times 10^8 M_\odot$, whereas Dean & Davies (1975) give the value as $8{\cdot}4 \times 10^8 M_\odot$. Any systematic flux density scaling errors can be revealed by comparing the flux density, S, at the peak of the H I profile measured by the different authors. In this respect, the present value $S = 3{\cdot}5 \pm 0{\cdot}12$ Jy is in closer agreement with the value $S = 3{\cdot}6 \pm 0{\cdot}5$ Jy (Rogstad *et al.* 1967) than with Dean & Davies's value of $S = 5{\cdot}8$ Jy, implying that their value for the overall H I mass may be too high.

[*facing page* 466]

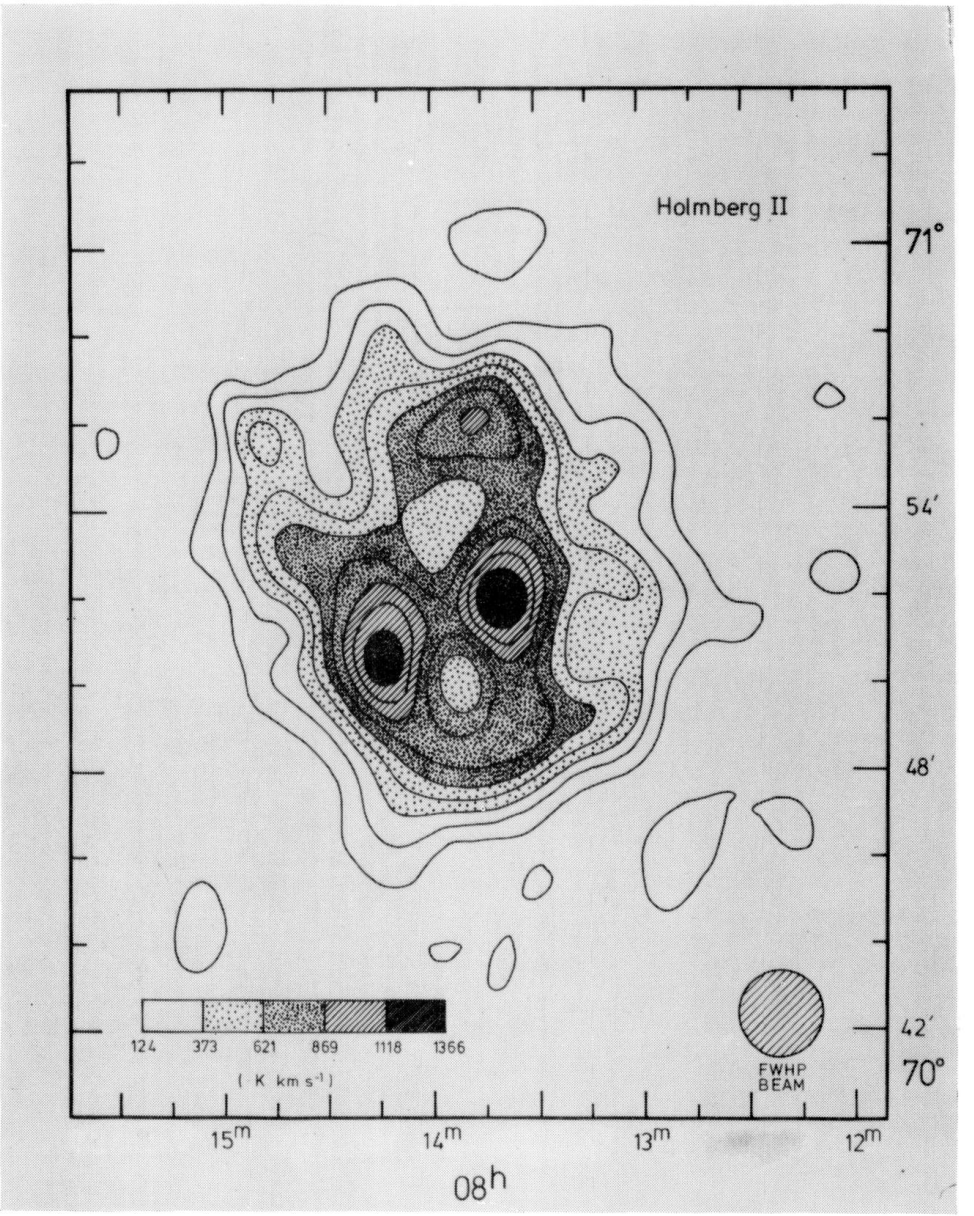

FIG. 1. *The integrated hydrogen contour map of Holmberg II. Contour levels are same as for Plate I. The H* I *dimensions are* 25–50 *per cent larger than the Holmberg dimensions.*

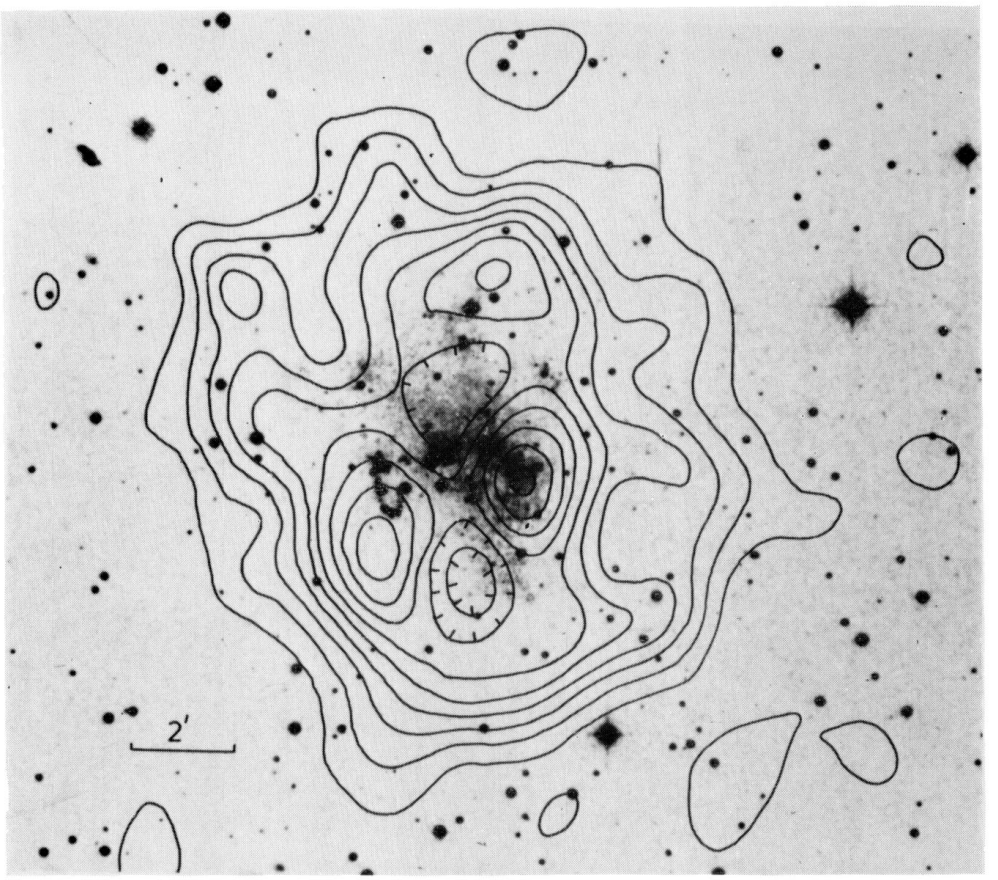

PLATE I. *A contour map of the integrated hydrogen emission superimposed on a blue print taken from the Palomar Sky Survey. The contour interval is* 124 *K km* s^{-1} *and the rms noise is* 92 *K km* s^{-1}.

A comparison of the surface densities of H I (σ_{HI}) and the stellar component (σ_S) is shown as a log–log plot in Fig. 5. The optical data were taken from the Hale telescope B plate (plate 20) of Sandage & Tammann (1974). Inside the plate area, $8'{\cdot}6 \times 6'{\cdot}4$, I counted 703 stellar images, and then compared the stellar surface density with that of the H I in the same region. Fig. 5 reveals a correlation between the surface densities. On the assumption that they are related by a power law of the form $\sigma_S \propto (\sigma_{HI})^n$, a least-squares fit to the data gave the value $n = 2{\cdot}3 \pm 0{\cdot}4$. This index is close to that found by Emerson (1974), $n = 2{\cdot}32 \pm 0{\cdot}11$, for the young H II

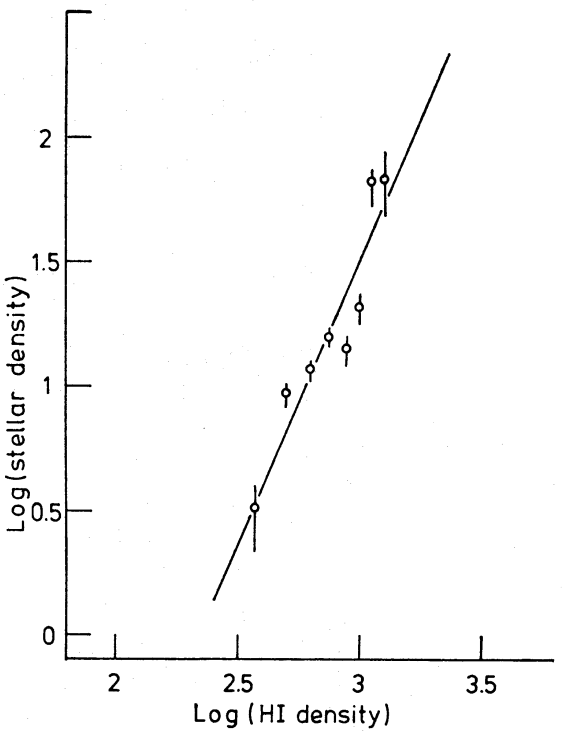

FIG. 5. *Projected stellar surface densities in Ho II against observed H I emission in the galaxy. The error bars reflect the statistical uncertainty. The straight line is the least-squares fit to the data and has a slope* $2{\cdot}3 \pm 0{\cdot}4$.

region associations in M31. The present result is also in agreement with Schmidt's (1959) conclusion that in our own Galaxy the rate of star formation varies as the square of the ambient gas density. The meaning of correlations of this type has been discussed by many authors—usually with conflicting conclusions. A recent review is given by Hamajima & Tosa (1975).

The limit on the continuum flux density inside the area of the faint (124 K km s^{-1}) outer H I contour (Fig. 1) was taken from the broadband map and is 1·5 mJy (beam area)$^{-1}$ which, if integrated over this area, gives a total upper limit of 68 mJy. This is in apparent contradiction with the claimed detection of a 400-mJy continuum source (Rogstad *et al.* 1967). However, there is a nearby continuum source at $\alpha_{1950{\cdot}0} = 08^h\,17^m\,05^s \pm 5^s$, $\delta_{1950{\cdot}0} = 71^\circ\,02'\,37'' \pm 5''$, of flux-density 430 ± 20 mJy. This source is only 20′ from the dynamical centre of Ho II, and therefore may have been confused with the galaxy by Rogstad *et al.*, whose beam size was 20′. The source is unresolved at the present angular resolution, and shows no absorption features in the radial velocity interval 92–237 km s^{-1}.

3.2 *The velocity field*

The radial velocity field is shown in Fig. 2 plotted inside the faint 124 K km s^{-1} contour taken from the integrated H I map. If Ho II has a true axial ratio $\epsilon_T = 0{\cdot}3$, like many irregular galaxies (Hodge & Hitchcock 1966), and an apparent axial ratio of 0·84, then assuming the galaxy to be an oblate spheroid implies an inclination of $i = 34°$. However, Holmberg (1950) gives the apparent axial ratio as $\epsilon_A = 1$, implying $i = 0°$. Therefore, in view of the uncertainty, the value $i = 20° \pm 10°$ has been adopted. The shape of the radial velocity contours indicates regular rotation and the adopted dynamical parameters are as follows:

Dynamical centre

$$\alpha_{1950{\cdot}0} = 08^h\ 13^m\ 56^s{\cdot}6 \pm 5^s$$

$$\delta_{1950{\cdot}0} = 70°\ 52'\ 7''{\cdot}0 \pm 5''.$$

Systemic velocity

$$V_S = 155 \pm 5 \text{ km s}^{-1}.$$

Inclination

$$i = 20° \pm 10°.$$

True axial ratio

$$\epsilon_T = 0{\cdot}3.$$

The rotation curve—Fig. 6(a)—has been constructed from radial velocities measured along the major axis and is uncorrected for inclination and beam-smoothing effects. The curve levels off at a radius $r \approx 2$ kpc from the centre, at a radial velocity of 20 ± 3 km s^{-1}. There is good agreement between the six independent points taken from each of the north and south portions of the major axis. The mean rotation curve was fitted with a sixth order polynomial in r (Burbidge, Burbidge & Prendergast 1959) and, in order to improve the accuracy of fitting, it was assumed to be Keplerian outside the radius of 7 kpc.

The total mass within a radius of 7 kpc is $M(7) = (4 \pm 1) \times 10^9\ M_\odot$ (the major error arising from the uncertainty in the inclination). If correction to other inclinations is required, the total mass will scale as $M(7) \propto \text{cosec}^2 i$. The ratio of overall hydrogen mass to $M(7)$ is $(M_{HI}/M(7)) = 0{\cdot}12 \pm 0{\cdot}09$. Dean & Davies (1975) quote a total B luminosity $L_B = 1{\cdot}2 \times 10^9\ L_\odot$, implying that the distance-independent ratio $(M_{HI}/L_B) = 0{\cdot}41 \pm 0{\cdot}02$ and the mass-to-light ratio $(M(7)/L_B) = 3{\cdot}2 \pm 1{\cdot}0$.

From the mass model adopted a number of interesting radially-dependent parameters can be evaluated. The variations of angular velocity, Ω, and epicyclic frequency, $K = 2\Omega(1 + (R/2\Omega)(d\Omega/dR))^{1/2}$ with radius have been derived from the rotation curve—Fig. 6(b). The value of the angular velocity $(\Omega - K/2)$ corresponds to the rate of precession of test particles making two radial oscillations per rotation period; it is < 6 km s^{-1} kpc^{-1} and fairly constant with radius. This value is close to that found in M33 by Warner, Wright & Baldwin (1973), i.e. 7 km s^{-1} kpc^{-1}.

The H I surface density in the line of sight was averaged in elliptical rings of axial ratio 0·84 and width 1′ centred on the dynamical centre, and is shown in Fig. 7(a), plotted against the distance along the major axis. The surface density of total mass $(\sigma_*)_\perp$, de-projected to a viewing angle perpendicular to the plane, is shown in Fig. 7(b), and the ratio of H I-surface-density to total-mass-surface-density perpendicular to the plane $(\sigma_{HI}/\sigma_*)_\perp$ in Fig. 7(c). Fig. 7(c) shows the ratio increasing to 30 per cent at a radius of 5 kpc and then decreasing outwards. The

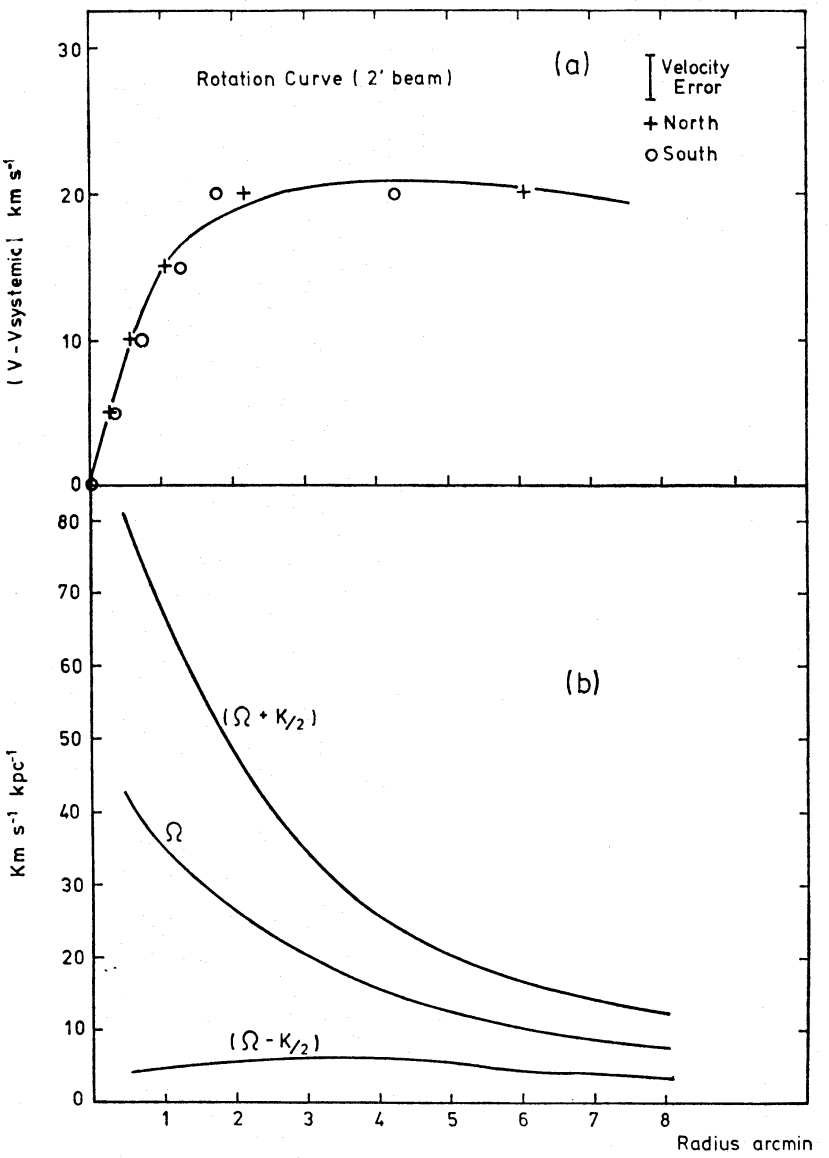

FIG. 6. *Curve (a) is the major axis rotation curve of Ho II (solid line) which has been adopted in the mass model of the galaxy (Section 3.2). The curve is uncorrected for beam-smoothing and inclination effects. (b) Shows the radial variations of angular frequency, Ω, and* $\Omega \pm K/2$ *where K is the epicyclic frequency.*

situation is different from that in M33 (Warner *et al.* 1973), for which the ratio rises monotonically. Because $(\sigma_*)_\perp$ is sensitive to the assumed rotation curve outside the measured range, a model in which the curve is assumed to remain *flat* out to 16 kpc is shown in Fig. 7(b) and (c)—curves (ii). The excess projected surface density in curve (b)—(ii) arises from the ellipsoidal shells of matter outside 7 kpc in the original Keplerian model—curve (i). It can be seen that there is still a turnover in $(\sigma_{HI}/\sigma_*)_\perp$ in case (ii).

3.3 *Integral properties*

The major integral properties of Ho II are shown in Table I. The overall spatial H I distribution is strikingly similar to that in the irregular galaxy IC 10 (Shostak

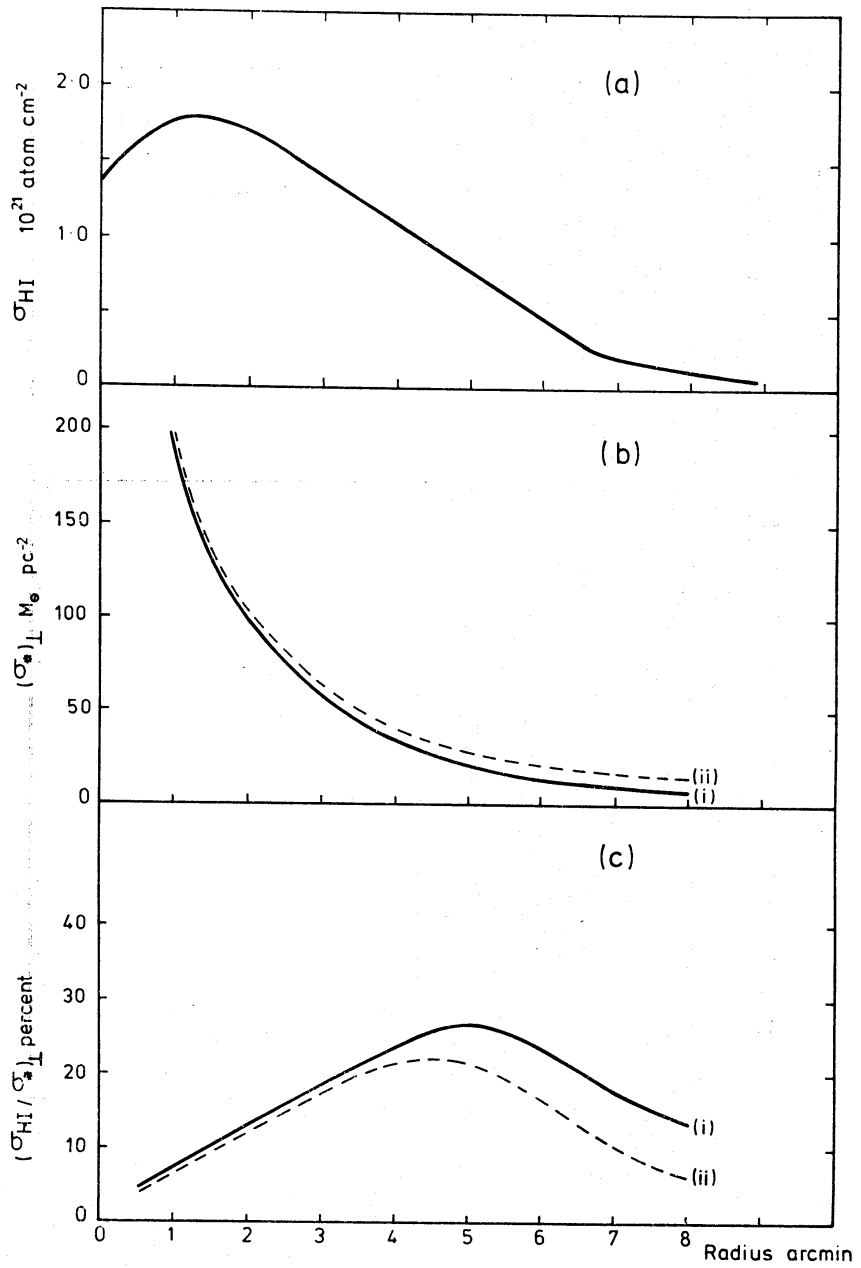

FIG. 7. *(a) is the mean projected surface density of H* I *averaged inside elliptical regions centred on the dynamical centre of the galaxy. (b) shows the de-projected total mass surface density in the mass model. (c) is the fractional surface density in the form of H* I*, de-projected to a viewing angle perpendicular to the plane. Curve (i) assumes a Keplerian rotation curve between 7 and 16 kpc whereas (ii) is based on a flat curve out to 16 kpc.*

1974), notably the wide extent of the H I compared to the optical image and the existence of large fluctuations in H I surface density near the central regions. In Table I, the total mass of Ho II is taken to be the value of M(7) derived in Section 3.2.

Apart from the differences in the 21-cm continuum flux density, the integral ratios are similar and this suggests that Ho II and IC 10 are in similar evolutionary states, with star formation in progress on scales ≈ 2 kpc.

TABLE I

The major integral properties of Ho II

Galaxy	Ho II	IC 10
Distance (Mpc)	3·22	3·0
Holmberg diameter	10′	9′·0 ± 3′·6
H I mass $M_{HI}/10^8\ M_\odot$	4·8 ± 0·2	10
Total mass $M/10^9\ M_\odot$	4 ± 1	5·4
Luminosity $L_B/10^9\ L_\odot$	1·2	3·5
M_{HI}/M	0·12 ± 0·09	0·19
M_{HI}/L_B	0·41 ± 0·02	0·29
M/L_B	3·23 ± 1·00	1·5
21-cm continuum flux density (mJy)	< 68	300 ± 80

4. INTERNAL DYNAMICS OF THE DENSE CONDENSATIONS

The dynamics of the condensations I and II are important because these appear to be associated with recent star formation. I is associated with an optically active region (Plate I) which also contains a relatively high surface density of blue stars (Sandage & Tammann 1974), whereas the peak projected surface density of H I in II lies close to a ' necklace ' of H II regions but is not associated with an excess of bright blue stars. The radial velocity dispersion map (Fig. 3) can be used to find the line-widths in these regions and hence information on their internal dynamical state. Because of the small inclination of Ho II, it is probable that the surface densities of H I in I and II are uncontaminated by ' background ' H I emission from the rest of the galaxy—an argument which also applies to the measurement of velocity dispersion.

The following dynamical measurements are based on a comparison of the virial masses (m_V) of condensations I and II with the known masses in the form of H I and stars (deduced from the mass model, assuming an axisymmetric distribution). If the observed FWHM of an H I profile in the direction of a condensation is ΔV km s^{-1}, the rms space–velocity dispersion is 0·74 ΔV km s^{-1} (assuming an isotropic distribution of velocities). The mean radii, r, were taken from the half-power dimensions, I being unresolved and II being partially resolved in declination. The density of neutral hydrogen was calculated assuming the condensations to be spherical. The mass required to bind a condensation gravitationally is the virial mass, $m_V = 0{\cdot}54(\Delta V)^2\, r/G$, and values of this and other relevant parameters appear in Table II.

From Table II it can be seen that only $\approx 0{\cdot}3$ of the binding mass is in the form of H I. However, the effect of the stars will be to increase the mass density inside the condensations and contribute to the ' missing mass '. In both condensations $(m_{HI}+m_*)/m_V \approx 1{\cdot}5$, suggesting that the mass in both stars *and* gas can give stability. If the optical depths are greater than unity then the m_{HI} are *underestimates* and the binding argument is strengthened. If the condensations are smaller than the beam then $m_V(\propto r)$ is reduced—again strengthening the argument.

Goldreich & Lynden-Bell (1965) have considered the growth of ' sheared condensations ' forming in a gaseous, isothermal disc with differential rotation. They found that short wavelengths are stabilized by pressure and long wavelengths by rotation. The critical density $\rho_0(0)$ for the formation of condensations with scale a few disc thicknesses was found to be $\rho_0(0) > 0{\cdot}7\, K^2/\pi G$. The constant 0·7 is

TABLE II

Values of the virial mass and other parameters

Condensation	I	II
Mean radius (pc)	900	950
$\bar{\rho}_{HI}$ (atom cm^{-3})	0·5	0·4
$\bar{\rho}_{*}$ (H atom cm^{-3})	2·0	2·0
$\bar{\rho}_{HI}/\bar{\rho}_{*}$	0·25	0·20
m_{HI} ($10^7 M_\odot$)	3·6	3·8
m_{*} ($10^7 M_\odot$)	14·3	18·8
ΔV (km s^{-1})	37	37
m_V ($10^7 M_\odot$)	12	13
m_{HI}/m_V	0·3	0·3
$(m_{HI}+m_{*})/m_V$	1·5	1·7

replaced by 0·6 under slightly different assumptions. This condition applies to ring-shaped condensations in which the motions are radial, but condensations are allowed to form where the contraction is tangential even when the gas is stable to radial contraction. Applying this condition to the condensations in Ho II, where at a radius $r = 2$ kpc the epicyclic frequency is $K \approx 40$ km s^{-1} kpc^{-1}, the predicted critical density is $\rho_0(0) = 2{\cdot}8\,H$ atom cm^{-3}, as compared to the observed gas density ($\approx 0{\cdot}5\,H$ atom cm^{-3}), and stellar density ($\approx 2{\cdot}0\,H$ atom cm^{-3}). The presence of stars may lead to gravitational instability even though the gas density does not satisfy the criterion. Given the fact that there are two 'holes' in the distribution at the same radius (2 kpc) as the condensations, it is interesting to speculate that the condensations may have resulted from a transverse instability of this kind.

ACKNOWLEDGMENTS

I thank members of the Radio Astronomy group for help with making these observations and in particular John Baldwin, John Shakeshaft and Barry Madore for useful comments on the manuscript.

REFERENCES

Baldwin, J. E., Field, C., Warner, P. J. & Wright, M. C. H., 1971. *Mon. Not. R. astr. Soc.*, **154**, 445.
Burbidge, E. M., Burbidge, G. R. & Prendergast, K. H., 1959. *Astrophys. J.*, **130**, 739.
Dean, J. F. & Davies, R. D., 1975. *Mon. Not. R. astr. Soc.*, **170**, 503.
de Vaucouleurs, G. & de Vaucouleurs, A., 1964. *Reference catalogue of bright galaxies*, University of Texas Press, Austin.
Emerson, D. T., 1974. *Mon. Not. R. astr. Soc.*, **169**, 607.
Goldreich, P. & Lynden-Bell, D., 1965. *Mon. Not. R. astr. Soc.*, **130**, 125.
Hamajima, K. & Tosa, M., 1975. *Publ. astr. Soc. Japan*, **27**, 561.
Hodge, P. W. & Hitchcock, J. L., 1966. *Publ. astr. Soc. Pacific*, **78**, 79.
Holmberg, E., 1950. *Medd. Lunds. astr. Obs.*, Ser. II, No. 128.
Kellermann, K. I., Pauliny-Toth, I. I. K. & Williams, P. J. S., 1969. *Astrophys. J.*, **157**, 1.
Rogstad, D. H., Rougoor, G. W. & Whiteoak, J. B., 1967. *Astrophys. J.*, **150**, 9.
Sandage, A., 1961. *The Hubble Atlas of Galaxies*, Carnegie Institution of Washington, Washington, DC.
Sandage, A. & Tammann, G. A., 1974. *Astrophys. J.*, **191**, 603.
Schmidt, M., 1959. *Astrophys. J.*, **129**, 243.
Shostak, G. S., 1974. *Astr. Astrophys.*, **31**, 97.
Warner, P. J., Wright, M. C. H. & Baldwin, J. E., 1973. *Mon. Not. R. astr. Soc.*, **63**, 163.